Microwave and Millimeter Wave Ferromagnetic Absorption of Nanoferrites

Liu Chao, Anjali Sharma, and Mohammed N. Afsar, *Fellow, IEEE*

Department of Electrical and Computer Engineering, Tufts University, Medford, MA 02155 USA

Complex dielectric permittivity and magnetic permeability of several commercially available nanoferrites have been studied over a broad microwave and millimeter wave frequency range. Nano-sized barium, strontium, copper, zinc, nickel substituted iron oxide powders with different lattice structures are investigated. A transmission-reflection based in-waveguide technique that employs a vector network analyzer was used to determine the scattering parameters for each sample in two microwave bands (18–40 GHz). A free space quasi-optical spectrometer energized by backward wave oscillators was used to acquire the transmittance spectra in the millimeter wave frequency range (30–120 GHz). Relatively broad and sharp ferromagnetic resonance of hexagonal barium ferrite and strontium ferrite are observed in millimeter wave frequency range. The ferromagnetic resonance peak for nano-sized hexagonal ferrite powder material moves to lower frequencies compared to micro-sized and solid hexagonal ferrites. An X-ray diffraction measurement is performed on these hexagonal ferrites to understand the magnetic behavior and the structure.

***Index Terms*—Dielectric permittivity, ferromagnetic resonance, magnetic domain, magnetic permeability, nanoferrite.**

I. Introduction

NANOFERRITES consist of metal substituted iron oxide nanopowders that have average particle size below 100 nm. These nanosize ferrites show different dielectric and magnetic properties in microwave and millimeter wave frequencies compared to micro-size and solid ferrites. Therefore there is a growing interest in studying these powders to understand how the material properties are affected by the particle size.

The use of nanoferrites is significant in many aspects, such as biological drug delivery systems, DNA-separators as well as in magnetic recording and information storage [1]. These nanosize ferrites are also useful in other microwave applications such as transformers, absorbers and circulators. It is necessary to investigate their electromagnetic properties and understand their changing magnetic behavior with particle dimension.

In the microwave measurement, a vector network analyzer together with waveguides was employed to determine the scattering parameters of the nanoferrites inside the waveguide in K band and Ka band. From the S-parameters, complex permittivity and permeability are evaluated by an improved algorithm. The millimeter wave measurement is based on a free space quasi-optical spectrometer powered by backward wave oscillators. Initially precise transmittance spectra over a broad millimeter wave frequency range from 40 GHz to 120 GHz are acquired. Later the transmittance spectra are converted into complex permittivity and permeability spectra. These ferrite powder materials are further characterized by x-ray diffraction (XRD) to understand the crystalline structure relating to the strength and the shift of the ferromagnetic resonance affected by the particle size.

II. Measurement Technique

A. Transmission-Reflection Waveguide

The transmission-reflection based waveguide technique has been widely used to determine the properties of solids. It can be further modified for the measurement of soft powders. The vector network analyzer measures the scattering parameters of the 2-port network formed by the waveguide shim filled with the sample under study as shown in Fig. 1.

The nanopowders were filled in the sample holder that was placed between the waveguides. It is important to ensure that the sample must fill the entire area of the sample holder so that there are no air gaps at the corners of the shim or between the powders. The sample was packed tight enough such that changing the orientation of the shim does not cause any shift in the particles.

The algorithm proposed by Baker-Jarvis was then used to derive the permittivity and permeability values from this data [2]. The phase unwrapping technique was employed to avoid the use of initial guess parameter [3]. Additionally, the cut-off frequency for each frequency band was calculated and set as the waveguide delay in the vector network analyzer to remove errors. The modified equations used in the measurements are given below,

$$\tilde{S}_{11} = \tilde{S}_{11} e^{j\left(0\times\sqrt{k_0^2-k_c^2}\right)}$$
$$\tilde{S}_{21} = \tilde{S}_{21} e^{j\left((l-d)\times\sqrt{k_0^2-k_c^2}\right)}$$

where l is the quarter wavelength difference between thru and line (in air), d is the thickness of the sample inside the waveguide, k_0 is the wavenumber of the sample and k_c is the cutoff wavenumber.

The final form of the equations used to determine permittivity and permeability is shown below

$$\varepsilon = -j\left(\frac{c}{f}\right)^2\left(\frac{1-\Gamma}{1+\Gamma}\right)\left(\frac{1}{2\pi d}\right)\left(\ln\left(\frac{1}{|T|}\right)+j(2\pi n-\varphi_T)\right)\times\left(\sqrt{\left(\frac{1}{\lambda_0}\right)^2-\left(\frac{1}{2a}\right)^2}\right)$$

$$\mu = \frac{\eta\gamma_{TE_{10}}}{j\gamma^0_{TE_{10}}} = -j\left(\frac{1+\Gamma}{1-\Gamma}\right)\left(\frac{1}{2\pi d}\right)\left(\frac{\ln\left(\frac{1}{|T|}\right)+j(2\pi n-\varphi_T)}{\sqrt{\left(\frac{1}{\lambda_0}\right)^2-\left(\frac{1}{2a}\right)^2}}\right)$$

where, Γ is the reflection coefficient, T is the transmission coefficient, $\gamma_{TE_{10}}$ and $\gamma^0_{TE_{10}}$ are propagation constant for the TE_{10} mode with and without the material inserted in the waveguide,

Manuscript received March 02, 2012; revised April 27, 2012; accepted May 15, 2012. Date of current version October 19, 2012. Corresponding author: L. Chao (e-mail: stream.chao@gmail.com).

Color versions of one or more of the figures in this paper are available online at http://ieeexplore.ieee.org.

Digital Object Identifier 10.1109/TMAG.2012.2200666

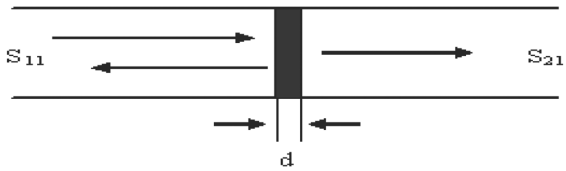

Fig. 1. Schematic diagram of nanoferrites in waveguide.

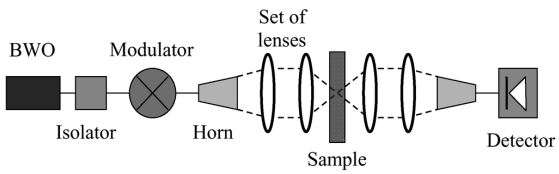

Fig. 2. Schematic diagram of the free-space quasi-optical millimeter-wave spectrometer in the transmittance mode with BWO as radiation source.

a is the longer dimension of the rectangular waveguide, ϕ_T is the phase of transmission coefficient and d is the material thickness.

B. Quasi-Optical Spectrometer

Free space millimeter wave quasi-optical spectroscopy technique, including technical details and measurement uncertainties analysis, has been successfully employed and presented by several researchers [4]–[7]. This study presents complex dielectric and magnetic measurements at millimeter waves performed by the free space quasi-optical spectrometer in transmittance mode [6], [7]. Three high vacuum, high power backward wave oscillators (also called carcinotrons) (BWO) have been used as sources of coherent radiation continuously tunable in the range from 30 to 120 GHz. A couple of pyramidal horn antennas and a set of polyethylene lenses along the propagation path from the source antenna to the receiver antenna have been adjusted to form a Gaussian beam as well as to focus the beam into the sample. The diameter of the millimeter wave beam focused into the sample has been found to be around a few millimeters. The simplified schematic diagrams of the millimeter wave quasi-optical spectroscopic system are shown in Fig. 2.

The mathematical relationships between transmittance and reflectance spectra, and refractive and absorption indexes are presented below

$$T = E\frac{(1-R)^2 + 4R\sin^2\psi}{(1-RE)^2 + 4RE\sin^2(\alpha+\psi)},$$

$$R = \frac{(n-1)^2 + k^2}{(n+1)^2 + k^2},$$

$$\varphi = \alpha + \arctan\frac{ER\sin^2(\alpha+\psi)}{1-ER\cos^2(\alpha+\psi)} + \arctan\frac{k}{n^2+k^2+n} - \arctan\frac{k}{n+1}$$

$$E = e^{-4\pi kdf/c}, \quad \alpha = \frac{2\pi ndf}{c}, \quad n+ik = \sqrt{\varepsilon^*\mu^*},$$

$$\psi = \arctan\frac{2k}{n^2+k^2-1},$$

where c is the speed of light, n is the refractive index of the sample material, k is the absorption index, μ is the complex magnetic permeability of the sample material, ε is the complex dielectric permittivity, T is the transmittance, R is the reflectance, φ is the phase of the transmitted wave, and ψ is the phase of reflected wave.

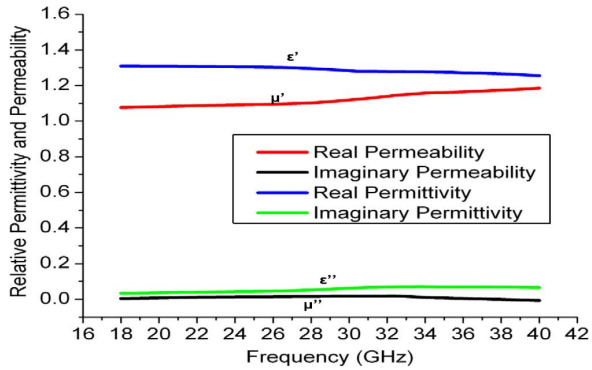

Fig. 3. Complex permittivity and permeability in K and Ka bands of Fe_4NiO_4Zn nanopowder. Real permeability is around 1.05 and the real permittivity is around 1.3. The imaginary part of permeability and permittivity are 0 and 0.05, respectively.

TABLE I
SAMPLE PREPARATION

Name	Chemical Formula	Purity	Density (g/cm^3)
Barium ferrite	$BaFe_{12}O_{19}$	99.9%	0.59
Strontium ferrite	$SrFe_{12}O_{19}$	99.8%	0.57
Copper iron oxide	$CuFe_2O_4$	98.5%	0.52
Copper zinc ferrite	$CuFe_4O_4Zn$	98.5%	0.55
Nickel zinc iron oxide	Fe_4NiO_4Zn	99%	0.28

III. SAMPLE PREPARATION

Five nanoferrites, namely barium ferrite ($BaFe_{12}O_{19}$, BaM), strontium ferrite ($SrFe_{12}O_{19}$, SrM), copper iron oxide ($CuFe_2O_4$, CAS-No.12018-79-0), copper zinc iron oxide ($CuFe_4O_4Zn$, CAS-No.66402-68-4), nickel zinc iron oxide (Fe_4NiO_4Zn, CAS-No.12645-50-0) examined in this work were purchased from Sigma Aldrich. The grain size of the powders varies from 40 nm to 100 nm for different kind of ferrites [8]. Density of the ferrites in the sample holder is determined by weighting from an accurate balance over the dimensions of the sample holders. The density and purity are listed in Table I.

IV. RESULTS AND DISCUSSION

Complex dielectric permittivity and magnetic permeability spectra obtained in microwave frequency range using transmission-reflection in-waveguide technique are shown below. Transmittance spectra of hexagonal ferrites are acquired in the millimeter wave frequency from 40 GHz to 120 GHz. The X-ray diffraction data are collected from 2θ angles from 5° to 70° in 0.015° step size on these hexagonal ferrite nanopowders.

The complex dielectric permittivity and magnetic permeability of nickel zinc iron oxide, copper zinc iron oxide and copper iron oxide nanopowder in 18–40 GHz frequency range are shown in Fig. 3, Fig. 4, Fig. 5, respectively. The real parts of permittivity (ε') of these copper, zinc, nickel substituted nanopowders are much smaller than their solid form. One can treat these nanopowders as diluted by the air between nano particles. The real part of magnetic permeability (μ') value is almost the same as the value for micro size and solid form. The imaginary parts of permittivity (ε'') values are close to zero for specifying to have high electric resistivity. No ferromagnetic resonance is observed in this frequency region for these samples and the imaginary parts of permeability (μ'') values are very small (close to 0.01 to 0.05).

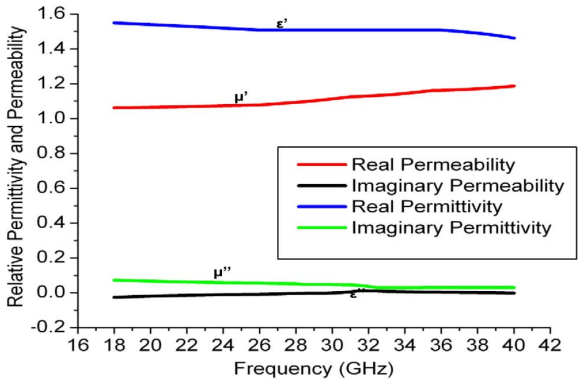

Fig. 4. Complex permittivity and permeability in K and Ka bands of $CuFe_4O_4Zn$ nanopowder. Real permeability is around 1.1 and the real permittivity is around 1.5. The imaginary part of permeability and permittivity are 0 and 0.05, respectively.

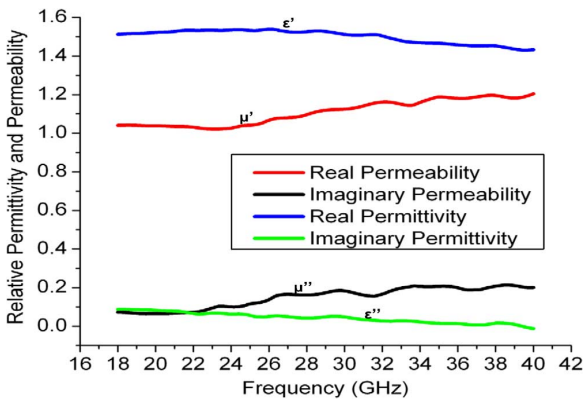

Fig. 5. Complex permittivity and permeability in K and Ka bands of $CuFe_2O_4$ nanopowder. Real permeability is observed in 1.0–1.2 region. The real permittivity varies around 1.5. The imaginary part of permeability and permittivity are 0.1.

TABLE II
SAMPLE AVERAGE PERMITTIVITY AND PERMEABILITY

Chemical Formula	μ'	μ''	ε'	ε''
$CuFe_2O_4$	1.12	0.12	1.47	0.06
$CuFe_4O_4Zn$	1.09	0.01	1.49	0.04
Fe_4NiO_4Zn	1.11	0.01	1.28	0.03

Table II shows the average permittivity and permeability of $CuFe_2O_4$, $CuFe_4O_4Zn$, Fe_4NiO_4Zn nanopowders in K and Ka bands from 18 GHz to 40 GHz.

Transmittance spectra of hexagonal barium (BaM) and strontium (SrM) nanoferrites measured by the quasi-optical technique are shown in Fig. 6. A deep and sharp absorption in transmittance spectra has been observed for both barium and strontium nanoferrites in 40–60 GHz frequency range. This deep absorption is the natural ferromagnetic resonance that shifts to millimeter wave range due to the strong magnetic anisotropy of barium and strontium ferrites. The periodic structure observed in all transmittance spectra at the frequencies above zone of deep absorption represents channel fringes. The analysis of channel fringes allows us to determine the complex dielectric permittivity value of materials.

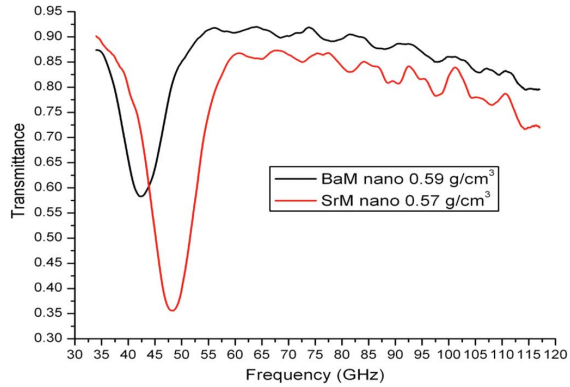

Fig. 6. Millimeter wave transmittance spectra of barium and strontium nanoferrites. Ferromagnetic resonance peaks are observed at 42.5 GHz and 48.2 GHz, respectively.

TABLE III
COMPLEX PERMITTIVITY AND RESONANT FREQUENCY

Chemical Formula	ε'	ε''	Resonant frequency	Theoretical Resonant frequency
$BaFe_{12}O_{19}$	1.88	0.01	42.5 GHz	48 GHz
$SrFe_{12}O_{19}$	2.15	0.01	48.2 GHz	52.5 GHz

TABLE IV
ANISOTROPY FIELD AND SATURATION MAGNETIZATION

Ferrite Size	Nano BaM	Solid BaM	Nano SrM	Solid SrM
H_A (kOe)	15.2	17.1	17.2	18.8
$4\pi M_s$ (kG)	0.07	0.37	0.12	0.38

To evaluate the complex magnetic permeability spectra, Schlömann's equation [9] for partially magnetized ferrites has been used:

$$\mu_{eff} = \frac{1}{3} + \frac{2}{3}\sqrt{\frac{(H_A + 4\pi M_s)^2 - \left(\frac{\omega}{\gamma}\right)^2}{H_A^2 - \left(\frac{\omega}{\gamma}\right)^2}}$$

where ω is the frequency, H_A is anisotropy field, $4\pi M_S$ is saturation magnetization, γ is the gyromagnetic ratio. Demagnetizing factors are determined by the theory of Schlömann's model for nonellipsoidal bodies. The complex permittivity and permeability together with the center of the ferromagnetic resonance are shown in Table III.

From the ferromagnetic resonance, the hexagonal barium and strontium nanoferrites show relatively strong anisotropy field of $H_A = 15.2$ kOe and $H_A = 17.2$ kOe and weak saturation magnetization of $4\pi M_S = 0.07$ kG and $4\pi M_S = 0.12$ kG, respectively. However, these anisotropy fields and saturation magnetization are smaller comparing to the solid barium and strontium ferrites which have anisotropy field of $H_A = 17.1$ kOe and $H_A = 18.8$ kOe, saturation magnetization of $4\pi M_S = 0.37$ kG and $4\pi M_S = 0.38$ kG, respectively. Comparison of anisotropy field and saturation magnetization between nano-sized and solid hexagonal ferrite is summarized in Table IV.

To understand the weak saturation magnetization is straightforward because the nanoferrites are actually diluted by the air between each particle even though the layer was compressed. The reduced anisotropy field is interesting for it is the intrinsic characteristic affected by the crystal structure. But the physical

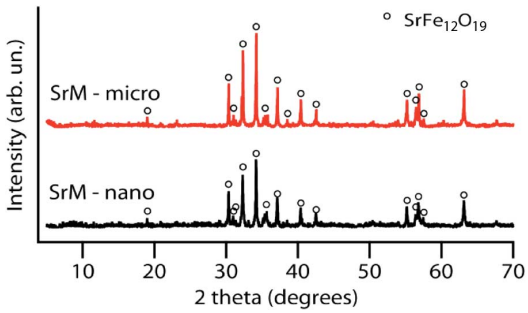

Fig. 7. XRD spectra for $SrFe_{12}O_{19}$ nanoferrite and micro-ferrite.

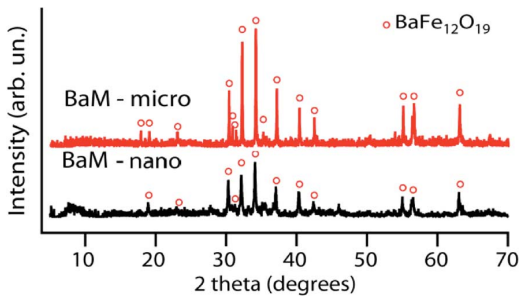

Fig. 8. XRD spectra for $BaFe_{12}O_{19}$ nanoferrite and microferrite.

change of the powder size does affect the anisotropy field of these hexagonal ferrites. The X-ray diffraction was then performed on this nanoferrites and the diffraction pattern is compared to micro size barium and strontium ferrites in Fig. 7 and Fig. 8.

The x-ray diffraction spectra show that both barium and strontium keep the same crystalline structure in micropowder and nanopowder particle size. This further demonstrates that the shifting of ferromagnetic resonance (towards lower frequency) and reduced anisotropy field are not caused by any crystal structure change. The micro size particle of the hexagonal ferrite has almost the same anisotropy field as the solid ferrite. This is due to the domain size of the hexagonal ferrite. The upper limit of single magnetic domain should have the size of about 100 nanometer.

The nanoferrite powder with a physical dimension smaller than this single magnetic domain size will lead to a lower ferromagnetic resonance frequency. At the upper limit of single domain size, all of the particle's internal magnetization is aligned to reduce the system energy to the lowest [10]. Therefore, at upper limit of single domain size, ferrite has the largest anisotropy field which is the sum of all magnetic moment in the particle. Below this physical upper limit of single domain size, the anisotropy field of the ferrite is determined by the volume of the particle until the dimension drops to a certain size. The spins of the magnetic moment will no longer be aligned without the application of an external magnetic field because of random thermal flips. As the powder dimension turns to even smaller size, the hexagonal ferrite is deduced to lose ferromagnetic resonance completely at room temperature. The size of barium and strontium nanoferrite powders measured in this paper is right between the upper limit of single domain size and the lower limit size of turning into superparamagnetism.

V. Conclusion

The complex dielectric permittivity and magnetic permeability are measured in microwave and millimeter wave frequency range. The improved vector network analyzer based transmission-reflection technique with waveguide is applied to several nanoferrites in microwave frequency. Quasi-optical backward wave oscillator spectrometer was employed to determine the transmittance of these nanoferrite samples. Ferromagnetic resonances on hexagonal barium and strontium nanoferrites are observed in the millimeter wave frequency range by this millimeter wave spectrometer. The ferromagnetic resonance is shifting to the lower frequency and the anisotropy field reduces to lower strength. X-ray diffraction was performed on these hexagonal nanoferrites. The diffraction spectra demonstrate that the crystal structure keeps the same as larger size barium and strontium ferrites. The ferromagnetic resonance moving is caused by magnetic domain size limit. Further research on the detail reasons leading to this phenomenon will be carried through.

References

[1] H. Pfeiffer, R. W. Chantrell, P. Görnert, W. Schüppel, E. Sinn, and M. Rösler, "Properties of barium hexaferrite powders for magnetic recording," *J. Magn. Magn. Mater.*, vol. 125, pp. 373–376, 1993.

[2] J. Baker-Jarvis, E. J. Vanzura, and W. A. Kissick, "Improved technique for determining complex permittivity with the transmission/reflection method," *IEEE Trans. Microw. Theory Tech.*, vol. 38, no. 10, pp. 1096–1103, Oct. 1990.

[3] N. N. Al-Moayed, M. N. Afsar, U. A. Khan, S. McCooey, and M. Obol, "Nano ferrites microwave complex permeability and permittivity measurements by T/R technique waveguide," *IEEE Trans. Magn.*, vol. 44, no. 10, pp. 1768–1772, Oct. 2008.

[4] A. A. Volkov, Y. G. Goncharov, G. V. Kozlov, S. P. Lebedev, and A. M. Prokhorov, "Dielectric measurements the submillimeter wavelength region," *Infrared Phys.*, vol. 25, pp. 369–373, 1985.

[5] G. V. Kozlov, S. P. Lebedev, A. A. Mukhin, A. S. Prokhorov, I. V. Fedorov, A. M. Balbashov, and I. Y. Parsegov, "Submillimeter backward-wave oscillator spectroscopy of the rare-earth orthoferrites," *IEEE Trans. Magn.*, vol. 29, no. 6, pp. 3443–3445, Nov. 1993.

[6] K. N. Kocharyan, M. Afsar, and I. I. Tkachov, "Millimeter-wave magnetooptics: New method for characterization of ferrites the millimeter-wave range," *IEEE Trans. Microw. Theory Tech.*, vol. 47, no. 11, pp. 2636–2643, Nov. 1999.

[7] K. A. Korolev, C. Shu, L. Zijing, and M. N. Afsar, "Millimeter-wave transmittance and reflectance measurement on pure and diluted carbonyl iron," *IEEE Trans. Instrum. Meas.*, vol. 59, no. 11, pp. 2198–2203, Nov. 2010.

[8] A. Sharma and M. N. Afsar, "Microwave complex permeability and permittivity measurements of commercially available nano-ferrites," *IEEE Trans. Magn.*, vol. 47, pp. 308–312, 2011.

[9] E. Schlomann, "Microwave behavior of partially magnetized ferrites," *J. Appl. Phys.*, vol. 41, pp. 1350–1350, 1970.

[10] E. C. Stoner and E. P. Wohlfarth, "A mechanism of magnetic hysteresis heterogeneous alloys," *Phil. Trans. Roy. Soc. Lond.. A, Math. Phys. Sci.*, vol. 240, pp. 599–642, 1948.